

Impact of Pulse Shapes on the Performance of an Ultra-Wideband Multiple-Access Fast Acquisition System

Yassine SALIH ALJ^{1,2*}, Charles DESPINS^{1,2,3}, *Senior Member, IEEE*,
and Sofiène AFFES^{1,2}, *Senior Member, IEEE*

1: INRS-E.M. & Telecommunications, 800, De La Gauchetière West, Suite 6900, Montreal (QC) H5A 1K6 Canada.

2: Underground Communications Research Laboratory (LRCS), 450, 3^d Av., Local 103, Val-d'Or (QC) J9P 1S2 Canada.

3: PROMPT-Quebec, 1010, Sherbrooke West, suite 1800, Montreal (QC) H3A 2R7 Canada.

Email: yassine@emt.inrs.ca; cdespins@promptquebec.com; affes@emt.inrs.ca

Abstract– Ultra-wideband (UWB) communication systems provide very high data rates by transmitting extremely short duration pulses. The impulse waveform is one of the key factors that influence the performance of these systems. While fulfilling the FCC spectral emission requirements, the pulse shape must offer high detection capabilities with suitable levels of accuracy. In this paper, we evaluate the effect of pulse shapes on the performance of an UWB computationally-efficient acquisition scheme in the presence of Multiple User Interference (MUI) and Gaussian noise. In the comparisons, different pulses with same duration were used in extensive Monte-Carlo simulations. Results show that the pulse shape has a noticeable impact on the performance of our UWB computationally-efficient acquisition scheme. Moreover, it is concluded that the 6th or the 8th order Gaussian derivative is the most suitable pulse shape to choose, depending on spectral bandwidth requirements.

Keywords– Ultra wideband, pulse shape, sequence acquisition.

I. INTRODUCTION

Ultra-wideband (UWB) radio is a fast emerging technology, currently regarded as an attractive solution for many wireless communication applications. As a carrier-free (baseband) wireless transmission technology, UWB radio utilizes ultra-short waveforms that are compatible with the FCC spectral masks. The resulting transmitted UWB signal is spread with a very low Power Spectral Density (PSD) over an absolute bandwidth of at least 500 MHz into a large spectrum (3.1-10.6 GHz) [1]. In addition to the PSD of the transmitted signal which is influenced by the used pulse shape, the performance of the UWB system itself may also be affected under non-ideal conditions [2]. Thus, the choice of the fundamental pulse shape used to generate an UWB signal is one of the most important considerations for an UWB system. In [3], the first ten Gaussian derivatives were compared in terms of their PSD and compliance to the FCC spectral constraints. For these pulses, higher-order derivatives have shown better fitting to the FCC masks with decreasing bandwidths as the order of the derivation increases. Indeed, as the pulse order increases, the number of zero crossings in the same pulse width also increases; the pulses begin to resemble sinusoids modulated by a Gaussian pulse-shaped envelope, thus corresponding to a

higher “carrier” frequency sinusoid modulated by an equivalent Gaussian envelope [2]. Moreover, Gaussian-based pulse shapes outperform generally other UWB typical pulse types, as recently proposed in [4], and are noticeably easier to generate [5]. These observations lead to considering Gaussian-based, typically high-order derivatives, as the most potential candidates for UWB systems.

In this paper, we evaluate the impact of different Gaussian-based pulses on an UWB computationally-efficient fast acquisition system. Considerable research effort has been devoted recently to accelerate the timing acquisition in UWB systems. Based on different algorithmic approaches, several rapid acquisition techniques, where the complexity aspect was generally less emphasized than the algorithmic one, were proposed [6-7]. In order to achieve a low-complexity receiver, an UWB computationally-efficient acquisition system showing explicit design characteristics that offer greatly improved computational cost and acquisition time was proposed in [8]. For this new UWB scheme based on a *Block-Processing* technique adapted to a FFT-based circular correlation, the pulse shape remains an important design factor to study in this paper. The performance levels of the first eleven Gaussian derivatives and the popular doublet waveform are compared in this paper to determine the most suitable pulse shapes to implement in the design of this typical fast acquisition scheme.

The remainder of this paper is organized as follows. In Section II, the characteristics of the Gaussian-based impulses are briefly highlighted and the used system concept is described. The considered UWB fast acquisition system is detailed in Section III. Section IV presents numerical results showing performance differences between impulse waveforms used within the fast acquisition system, and Section V concludes the paper.

II. SYSTEM MODEL

Direct-Sequence (DS) UWB concept is employed for the system considered in this paper with BPSK pulse signaling. The transmitted pulse shape used within an UWB system influences its spectral properties. However due to the antenna

effect, the processed pulse at the receiver is modeled as a derivation of the used transmitted pulse shape. The basic Gaussian pulse is expressed as

$$p(t) = \frac{1}{\sqrt{2\pi\sigma}} \exp\left(-\frac{t^2}{2\sigma^2}\right), \quad (1)$$

where σ is a shape factor used typically as a bandwidth decaying parameter. The n^{th} order Gaussian derivative can be determined recursively from

$$p_n(t) = -\frac{n-1}{\sigma^2} p_{n-2}(t) - \frac{t}{\sigma^2} p_{n-1}(t). \quad (2)$$

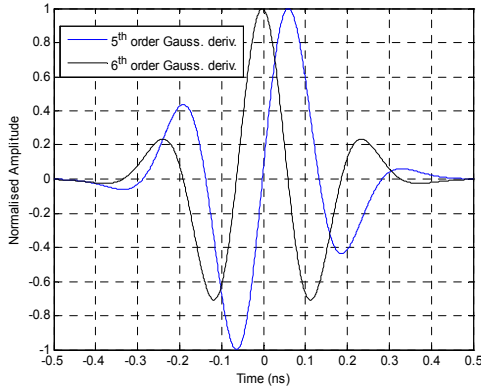


Fig. 1. 5th and 6th order Gaussian derivatives pulse shapes in time domain.

The amplitude spectrum of the n^{th} order Gaussian derivative, obtained from its Fourier transform, is

$$|X_n(f)| = (2\pi f)^n \exp\left\{-\frac{(2\pi f\sigma)^2}{2}\right\}. \quad (3)$$

By differentiating (3) and setting it equal to zero, the peak emission frequency f_p , at which the maximum is attained, can be found satisfying the following:

$$2\pi f_p \sigma = \sqrt{n}. \quad (4)$$

Then, the Gaussian derivatives of higher orders are characterized by higher peak frequency while reducing the shape factor σ shortens the pulse. Notice that the PSD of the first order Gaussian derivative doesn't meet the FCC requirement no matter what value of the pulse width is used. Moreover, increasing the order of the derivative results in a wider overall pulse width for each successive pulse and, consequently, a narrower bandwidth around the same center frequency, thereby showing better fitting to the FCC masks.

In the used DS-UWB system the pulse occupies the entire chip interval and is transmitted continuously according to a MLS spreading code. The DS-UWB signal transmitted by a user k can typically be expressed as

$$s_{tr}^{(k)}(t) = \sum_{j=-\infty}^{j=+\infty} \sum_{n=0}^{N_c-1} d_j^{(k)} \cdot c_n^{(k)} \cdot p_{tr}(t - jT_f - nT_c), \quad (5)$$

where $p_{tr}(t)$ represents the transmitted *monocycle* pulse, $\{d_j\}$ the modulated data symbols mapped into $\{-1, 1\}$, $\{c_n\}$ are the spreading chips generated according to a MLS code, T_c is the chip duration, and there are N_c chips per each message symbol j of period T_f – the spreading factor – such that $N_c \cdot T_c = T_f$. When N_u users are active while focusing on the first transmitter, the received signal can be modeled as

$$r(t) = s_{pr}^{(1)}(t - \tau) + n_{tot}(t), \quad (6)$$

where τ is the phaseshift between the transmitter and the receiver and $n_{tot}(t)$ is

$$n_{tot}(t) = \sum_{k=2}^{N_u} s_{pr}^{(k)}(t) + n(t), \quad (7)$$

in which $s_{pr}(t)$ corresponds to $p_{pr}(t)$, the processed pulse shape at the receiver (antenna effect) and where $n(t)$ represents the receiver noise modeled as $N(0, \sigma_n^2)$ with a power spectral density of $N_0/2$. The interfering users are assumed to be perfectly synchronized. Furthermore, as the signals are transmitted over a wireless link, the frame duration is considered far smaller than the channel's coherence time, which means that the fading is quite constant over a large number of frames.

III. UWB FAST ACQUISITION SYSTEM

For fast and accurate acquisition of UWB signals with optimal receiver complexity, the *Block-Processing* technique was used with an *FFT-based high-speed* frequency correlator. Synchronization is performed by an FFT-based circular correlator fed by the processed blocks. The block length M is taken as of power-of-two; thus the FFTs have an optimal butterfly structure. Therefore, the correlation is computed in the frequency domain by a simple multiplication, producing the same result as the standard correlation but faster with this high-speed correlation technique. The block diagram of the considered UWB fast acquisition system is shown in Fig. 1. For a sampling rate $F_s = 8$ Gsps used over a spreading factor $N_c = 63$ and a pulse duration $T_p = T_c = 2$ ns (duty cycle of 100%), the acquisition process is accelerated by handling the dense DS-UWB signal in simultaneous blocks of samples and by reducing the computational cost by a factor of 32 [8]. The processed DS-UWB received signal can be modeled as

$$r_{i,\mu}^{(j,N_u)} = d_{u,\tau_i}^{(j,k)} c_{i,\tau_i}^{(j,k)} p_{pr} \left((m_i + u) - jT_f - \frac{N_c}{M} (m_i + u) T_c - \tau_i \right) + n_{tot(i,\mu)}^{N_u}, \quad (8)$$

where u refers to the u^{th} sample ($u = 1, 2, \dots, M$) of the i^{th} block, m_i the total number of samples before the i^{th} block ($m_i = (i-1) \cdot M$) and where k corresponds to the acquired user at the receiver. For each acquired block i , the correlation is computed in the

frequency domain by a simple multiplication, while a code-phase τ_i and a Signal to Interference plus Noise Ratio $SINR_i$ are estimated.

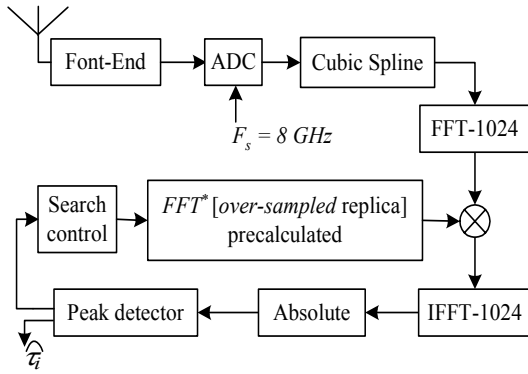


Fig. 2. Block diagram of the UWB fast acquisition system.

As shown in Fig. 1, a *cubic spline interpolation* is used as an *over-sampling* method to increase the cardinality of the blocks, digitized by the ADC converter, from 1008 samples to $M=(N_c+1) \cdot T_c \cdot F_s=1024$ (*i.e.* power-of-two) in order to make possible the use of FFTs with butterfly structure. The FFT used for the local pulse-train MLS code-replica is pre-calculated so that only one FFT/IFFT pair is used in the fast correlator structure. A peak detector examines its outputs (*i.e.* 1024 inverse-FFT outputs) to evaluate the detected peak amplitude and to deduct its position τ_i . If no peak was detected, the search control block leads the local code generator index to the next pre-calculated replica $k+1$. It was noticed that the over-sampling technique changes the overall correlation properties (*e.g.* peak amplitude) of the pulse shape [8]. Hence, the pulse shapes will behave herein differently in comparison to other time-domain acquisition systems.

IV. SIMULATION RESULTS

To assess and compare the performance of the used pulse shapes within the DS-UWB fast acquisition system, numerical simulations were carried out. We present in this section results obtained for the first eleven Gaussian derivatives and the doublet waveforms. To ensure an effective bandwidth of at least 500 MHz, the common pulse width is taken equal to 2 ns. Under Gaussian noise and MUI, a phase-shift of 60 ns is preset between the transmitter of interest and the receiver with a tolerated time-shift error threshold equal to 4 ns.

Figs. 3 and 4 show when, respectively, the noise variance and MUI levels increase the performance degradation of the simulated pulse shapes in terms of correlation peak amplitude (*i.e.* obtained normalized $SINR$) and phase-shift estimation error. These performance indices correspond to the overall detection capabilities as the BER cannot be quantified when despreading since an absolute operation is applied at the complex outputs of the fast correlator. Random and large data vectors were used in Monte-Carlo simulation technique to compute the performance degradation. The number of samples has been chosen equal to 10^5 , and the noise variance was taken $\sigma_n^2=2$ in the MUI case. In addition, the PN sequences were

randomly selected from the six best m-sequences of period 63 chips.

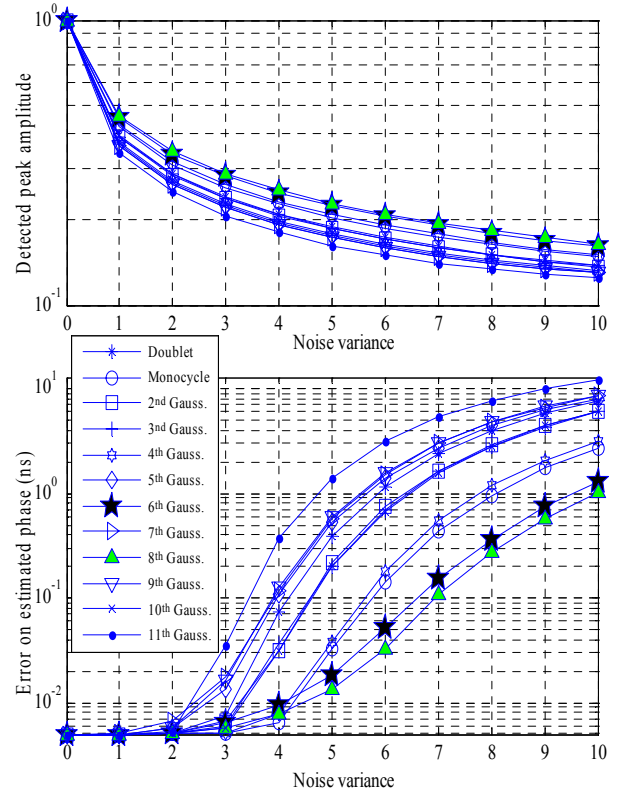


Fig. 3. Performance comparison under Gaussian noise without MUI.

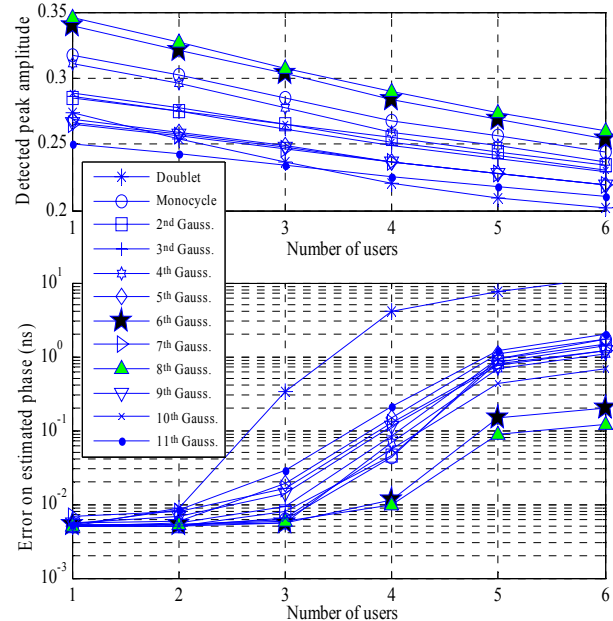


Fig. 4. Performance comparison under MUI and noise ($\sigma_n^2=2$).

From the results, we notice that the best performance score is obtained by the 8th Gaussian derivative and a bit lower level with the 6th-order derivative. We note also a more severe impact of the MUI on the doublet pulse shape. It was noticed

for the three first order derivatives, irrespective to their performance, these pulses do not meet the FCC spectral masks [9] and cannot satisfy it, irrespective of the pulse duration. Therefore, it is concluded that the 6th or the 8th order Gaussian derivative is the most suitable pulse shape to choose, depending on the spectral bandwidth requirements, since the 6th derivative offers a wider bandwidth. Indeed, as derivative order increases, the peak emission frequency increases and signal bandwidth decreases. Hence, choosing the most appropriate derivative order is a trade-off with pulse shape factor for a desired performance level. Bandwidth maximization is also an important factor in choosing the derivative order of the UWB pulse transmission [5]. Keeping this point in consideration, the 6th order Gaussian derivative has been chosen for this proposed UWB fast acquisition system.

V. CONCLUSION

In this paper, the effect of pulse shapes on the performance of a new UWB fast acquisition scheme has been evaluated in the presence of Multiple User Interference and Additive Gaussian Noise. Different Gaussian-based pulses were compared in extensive Monte-Carlo simulations. The Results have shown that the pulse shape have a clear impact on the performance of the studied UWB computationally efficient acquisition system and it was concluded that the 6th and the 8th order Gaussian derivatives are the most suitable pulse shapes to adopt in this scheme, depending on spectral bandwidth requirements. Moreover, taking into account the spectral

bandwidth maximization as an important design factor, the 6th order Gaussian derivative has been chosen in this study.

REFERENCES

- [1] Federal Communications Commission "Revision of part 15 of the commission's rules regarding ultra-wideband transmission systems," First Report and Order, ET Docket 98-153, April 2002.
- [2] M. Welborn and J. McCorkle, "The importance of fractional bandwidth in ultra-wideband pulse design," *Proc. IEEE Int. Conf. Communications*, vol. 2, pp. 753-757, April 2002.
- [3] H. Sheng, P. Orlik, A.M. Haimovich, L.J. Cimini, and J. Zhang, "On the spectral and power requirements for ultra-wideband transmission," *Proc. IEEE Int. Conf. Communications*, vol. 1, pp.738-742, May 2003.
- [4] B. Hu and N.C. Beaulieu, "Pulse shapes for ultrawideband communication systems," *IEEE Trans. on Wireless Communications*, vol. 4, pp. 1789-1797, July 2005.
- [5] M.U. Mahfuz, K.M. Ahmed, R. Ghimire and R.M.A.P. Rajatheva, "Performance Comparison of Pulse Shapes in STDL and IEEE 802.15.3a models of the UWB Channel," *Proc. IEEE ICICS'05*, pp.811-815, December 2005.
- [6] S.R. Aedudodla, S.Vijayakumaran and T.F.Wong, "Timing acquisition in ultra-wideband communication systems," in *IEEE Trans. on Vehicular Technology*, vol. 54, pp.1570-1583, September 2005.
- [7] L. Reggiani and G. M. Maggio, "Rapid search algorithms for code acquisition in UWB impulse radio communications," in *IEEE Journal on Selected Areas in Comm.*, vol. 23, no. 5, pp. 898-908, May 2005.
- [8] Y. Salih-Alj, C. Despins, and S. Affes, "A computationally efficient implementation of a UWB fast acquisition scheme," *Proc. IEEE VTC'07-Spring*, April 2007, in press.
- [9] L.L. Zhou and H. Zhu, "Waveform design and performance analysis of ultra-wideband (UWB) pulse based on iterative algorithm," *Proc. IEEE CEEM'06*, pp. 755-758, August 2006.